CHAPTER

CARBON CONTAINING NANOSTRUCTURED POLYMER BLENDS

10

Oluranti Agboola[*,†], Emmanuel Rotimi Sadiku[†], Tauhami Mokrani[*]

Department of Civil and Chemical Engineering, University of South Africa, Johannesburg, Republic of South Africa[*]

Department of Chemical, Metallurgical and Materials Engineering, Tshwane University of Technology, Pretoria, Republic of South Africa[†]

CHAPTER OUTLINE HEAD

10.1 INTRODUCTION

Carbon occurs in many forms, and their properties, depending on each form of its special structure, make carbon a truly unique building block for nanomaterials. Nanocarbon materials are defined so that not only is their primary particle size on a nanometer scale, but also their structures and/or textures are controlled on a nanometer scale [1]. Either the nanosize or nanostructure of the carbon materials have to be deliberately controlled to govern their properties and functions [2]. In the last two decades, novel

Design and Applications of Nanostructured Polymer Blends and Nanocomposite Systems. http://dx.doi.org/10.1016/B978-0-323-39408-6.00009-1

nanostructures have emerged, such as fullerenes, carbon nanotubes (CNTs), and graphene [3]. The flat monolayer of sp^2 carbon atoms are tightly packed into two dimensional honeycomb-like lattices which are the building blocks for graphene. Carbon has been used in various areas of nanosize research, such as electronics, sensors, super capacitors, batteries, fuel cells, and biosensors [4–9] because of its remarkable mechanical, optical, thermal, magnetic, and electronic [10–14] properties.

CNTs are known as allotropes of carbon with a cylindrical nanostructure and have novel properties that make them potentially useful in a wide variety of applications in nanotechnology. Their appearance is that of rolled tubes of graphite, such that their walls are hexagonal carbon rings, and they are often formed in large bundles. The ends of CNTs are domed structures of six-membered rings, capped by a five-membered ring [15]. Graphene is very similar to CNTs; they are both composed of carbon atoms linked together. The difference is that graphene is a flat layer of carbon, only one atom thick, where nanotubes are carbon atoms rolled up into a tube shape. The great strength that nanotubes are known for is as a result of the bonds between carbon atoms. Those same bonds ensure that graphene is also a very strong material. Nanotubes are members of the fullerene structural family; their name was derived from their long, hollow structure with the walls formed by one atom thick sheet carbon called graphene. These sheets are rolled at specific and discrete "chiral" angles and the combination of the rolling angle and the radius decides the nanotube properties (whether the individual nanotube shell is metal or semiconductor). CNTs can be classified as single-walled CNTs (SWCNTs), individual cylinders consisting of a single rolled graphene sheet and multiwalled CNTs (MWCNTs), a "Russian doll" structure constituting several concentric graphene cylinders, with weak Van der Waals forces binding the tubes together [15,16]. The various ways of rolling graphene into tubes are described by the tube chirality, i.e., the angle of the orientation of graphene sheet relative to the axis of the tube. The wall of CNTs is composed of one or multiple layers of graphene sheets; thus, it is possible to discriminate these materials in SWCNTs, formed by rolling up of a single graphene sheet and MWCNTs, formed by rolling up of more than one graphene sheet. Both SWCNTs and MWCNTs are capped at both ends of the tubes in a hemispherical arrangement of carbon networks called fullerenes warped up by the graphene sheet as shown in Figure 10.1 [17]. The interlayer separation of the graphene layers of MWCNTs is about 0.34 nm on average, each one forming an individual tube and the outer diameter ranging from 2.5 to 100 nm, while for SWCNTs this value ranges from 0.6 to 2.4 nm. The chemical bonding of nanotubes is made up of sp^2 bonds, which are similar to those of graphite.

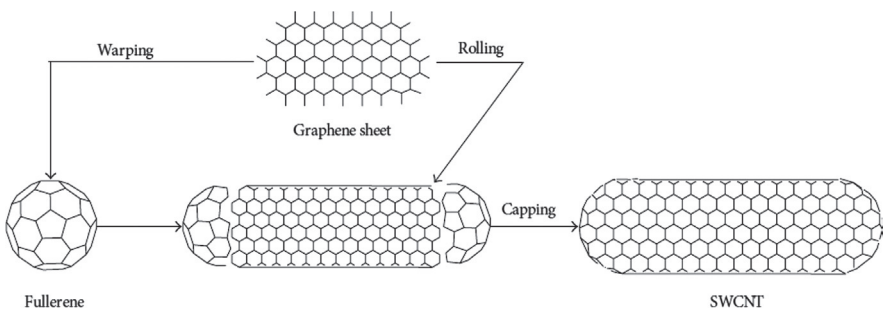

FIGURE 10.1

Molecular structure of graphene sheet, SWCNTs and MWCNTs [17].

10.2 DIFFERENT CATEGORIES OF CARBON NANOSTRUCTURE

The categories of nano-sized materials are quite challenging because of the intensive heterogeneity of their compositions and shapes. Different approaches can be used to classify carbon nanostructures; the suitable classification devise solely depends on the field of application of the nanostructures. One approach assumes as the basis of classification the characterization of the size of nanostructured. This approach covers not only nano but also microscopic carbon materials, such as carbon fiber [18]. One can also, for example, base a classification on an analysis of the dimensionalities of the structures [19–21], which in turn are connected with the dimensionality of quantum confinement and, thus, are related to nanoelectronic applications [21]. The entire range of dimensionalities is represented in the nanocarbon world, beginning with zero dimension structures (fullerenes, diamond clusters) and includes one-dimensional structures (nanotubes), two-dimensional structures (graphene), and three-dimensional structures (nanocrystalline diamond, fullerite) [22]. Stone and Glass [23] reported a classification of carbon nanostructures based on the dimensional organization of their edge structures. Morphological benchmarks of the classification are provided, including a novel graphenated CNT hybrid which increases the linear edge density of nanostructured carbons by an order of magnitude. Geometric consideration of the dimensional nature of the edge organization enables quantification of the edge density per unit nominal area. By classifying nanostructures based on linear edge density, a deeper understanding of materials performance can be obtained and a more informed comparison of nanostructures is enabled.

10.3 CNT AND GRAPHENE REINFORCED POLYMER COMPOSITE

Composites consist of a high-modulus fiber in a low-modulus matrix, where the fiber toughens and strengthens the binding material, or matrix. Due to their exceptional mechanical properties, SWCNT are commonly used as the reinforcing fiber in CNT composite [24,25]. CNTs have various chiralities in the graphene lattice which define the tube structure (see Figure 10.2) [26]. The angle of twist is directly related to the chiral vector (C_h) which is defined by the vector addition of two normalized (unit) vectors, a_1 and a_2, and their respective indices (m, n) as shown in Equation (10.1):

$$C_h = na_1 + ma_2 \tag{10.1}$$

CNTs (cylindrical nanostructures of carbon) and graphene (a single atomic layer of graphite) are revolutionizing technology and nanotechnology. Carbon-based nanofillers, such as carbon black, exfoliated graphene (EG), CNT, and carbon nanofiber (CNF) have recently been introduced to the preparation of polymer nanocomposites [27–34,11,35–43] with a suitable polymer matrix. The different shapes and structures of these conductive fillers and the morphologies of their dispersion will affect the ability to construct an effective conductive network, which is aimed at increasing the electrical conductivity of the polymer-filler composites. Among nanofillers, CNTs have proven to be very effective as conductive fillers [37,44–47]. The only drawback of CNTs as nanofiller is their higher production cost [48]. The mass production of CNT-based functional composite materials is thus very difficult.

Investigations have shown that polymer composite with single-walled carbon nanotubes (SWCNTs) as filler provides −40 dB electromagnetic interference (EMI SE) at 10 GHz [49]. Literature reveals that

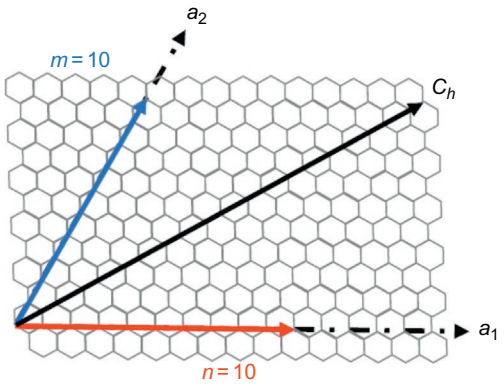

FIGURE 10.2

(10, 10) Armchair nanotube chiral vector diagram [26].

short-carbon-fiber-filled composites also yielded −40 dB (EMI SE) at 10 GHz and it was reported to be more effective than MWCNTs and carbon black filled composites [50]. Carbon black and CNTs have been simultaneously introduced into polymer matrices through conventional processing techniques [32,47,51–53]. The application of coiled CNTs has been found to be more effective than the use of conventional CNTs, giving only −15 dB at 8 GHz [54]. From the survey of polymer-based nanocomposites, results are varying dependent on several factors from the type of the polymer matrix to filler type and amount.

In nanocomposites, graphene improves the strength and conductivity of many thermosetting polymers. It is considered a two-dimensional carbon nanofiller with a one-atom-thick planar sheet of sp^2 bonded carbon atoms that are densely packed in a honeycomb crystal lattice. It is also regarded as the "thinnest material in the universe" with tremendous application potential [55]. Graphene is predicted to have remarkable properties, such as high thermal conductivity, superior mechanical properties and excellent electronic transport properties [56–58]. Some researchers studied EMI shielding of exfoliated graphite in a polymer matrix at different frequency ranges and produced different shielding efficiencies [59–63]. The excellence properties of graphene when compared to polymers are also shown in polymer/graphene nanocomposites. Polymer/graphene nanocomposites possess high electrical, thermal, mechanical, gas barrier, and flame retardant properties when compared to polymer [33,63–70].

Some researchers reported that the improvement of electrical and mechanical properties of graphene-based polymer nanocomposites performs better in comparison to that of clay or other carbon-filler-based polymer nanocomposites [71–73]. Although CNTs show comparable mechanical properties compared to graphene, still graphene is a better nanofiller than CNT in certain aspects, such as thermal and electrical conductivity (see Table 10.1) [55]. However, an improvement in the physicochemical properties of the nanocomposites depends on the distribution of graphene layers in the polymer matrix as well as interfacial bonding between the graphene layers and the polymer matrix. Interfacial bonding between graphene and the host polymer dictates the final properties of the graphene reinforced polymer nanocomposite [55].

Polymer nanocomposite development has been a sensitive area of research and has evolved significantly over the last two decades because of the ability of nanoscale reinforcements to create remarkable

Table 10.1 Properties of Graphene, Carbon nanotube, Nano-Sized Steel, and Polymers [55]

Materials	Tensile Strength	Thermal Conductivity at Room Temperature (W/mk)	Electrical Conductivity (S/m)
Graphene	130 ± 10 GPa	$(4.84 \pm 0.44)*10^3$ to $(5.30 \pm 0.48)*10^3$	7200
Carbon nanotube	60-150 GPa	3500	3000-4000
Nano-sized steel	1769 MPa	5-6	1.35×10^6
Plastic (HDPE)	18-20 MPa	0.46-0.52	Insulator
Rubber (natural rubber)	20-30 MPa	0.13-0.142	Insulator
Fiber Kevlar	3620 MPa	0.04	Insulator

property enhancements at relatively low filler concentrations, compared to conventional composites. The growth of different types of nanomaterials such as nanoclays, CNFs, CNTs, graphenes, nano-oxides like nanoalumina, nanosilica, titanium dioxide has resulted in the development of composites with exceptionally attractive macroscopic multifunctional properties in most circumstances depending on their inherent characteristics. Excellent electrical, thermal, mechanical, optical, fire-retardant, barrier, antibacterial, and scratch resistant properties of these composites have been reported and the results are only getting better with time [64–69]. The high surface-area-volume ratio of these fillers facilitates the attainment of desired macroscopic functionality at substantially lower filler loading fractions [74]. The relationship between processing, structure, and property of polymer/CNT composite materials and polymer/graphene composite materials will be discussed

10.3.1 RELATIONSHIP BETWEEN PROCESSING, STRUCTURE, AND PROPERTY OF POLYMER/CNTs COMPOSITE MATERIALS

There are remarkable improvements in the electrical and mechanical properties of composite materials, when CNTs are used as fillers instead of other conventional materials. CNTs performs better than the other carbon-based fillers like CNFs which require higher filler loading fractions to exhibit similar levels of electrical conductivity. Continuously lowering costs of CNTs, especially MWCNTs together with increases in demand and production capabilities augments favorably for a huge polymer-CNT nanocomposite market [74]. When discussing polymer/CNT composites, two major classes come to mind. First, the CNT nanofillers are dispersed within a polymer at a specified concentration, and the entire mixture is fabricated into a composite. Secondly, as-grown CNTs are processed into fibers or films, and this macroscopic CNT material is then embedded into a polymer matrix [75]. The four major fiber-spinning methods used for polymer/CNT composites from both the solution and melt include dry-spinning [76–78], wet-spinning [79], dry-jet wet spinning/gel-spinning [80], and electrospinning [81,82] is shown in Figure 10.3.

In spite of these processing techniques, many parameters need to be well controlled in order to develop high-quality fibers. Generally, all spinning procedures involve (i) fiber formation, (ii) coagulation/gelation/solidification, and (iii) drawing/alignment. The even dispersion of the CNT within the polymer solution or melt is very important for all these processes. To date, controlled dispersion of CNTs in a solution or a composite matrix remains a challenge, due to the strong Van der Waals

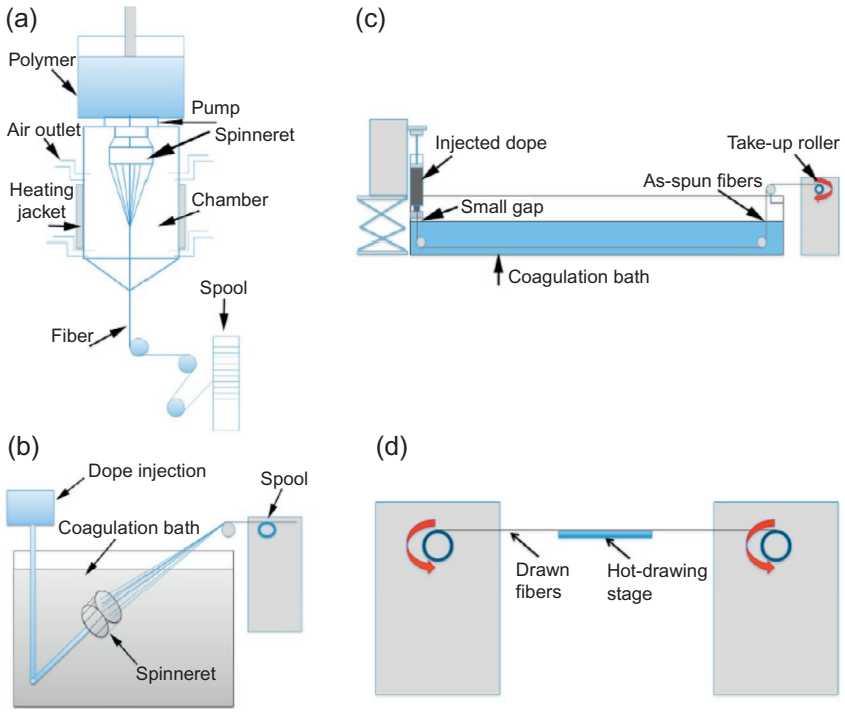

FIGURE 10.3

Schematics representing the various fiber processing methods (a) dry-spinning, (b) wet-spinning, (c) dry-jet wet or gel-spinning, and (d) postprocessing by hot-stage drawing [75].

binding energies associated with the CNT aggregates [83]. However, in terms of achieving excellent axial mechanical properties, alignment and orientation of the polymer chains and the CNT in the composite is necessary. Fiber alignment is accomplished in postprocessing such as drawing/annealing and is the key to increasing crystallinity, tensile strength, and stiffness [84].

10.3.1.1 The uses of CNTs as nucleating agent in polymer composite fibers

The nucleating agents can be mainly divided into three kinds: inorganic additives, organic additives, and polymers [85]. Nucleating agents for polymer crystallization is a very important aspect in the processing of polymer/CNT fibers. The nucleating effect on polymer crystallization depends on several aspects, such as the size and the geometry of the particles, the surface structure, and interfacial interactions with the polymer matrix. CNTs are the best nucleating agent, particularly SWCNT. The fabricating polymer/CNT composites initially focused on achieving mechanical properties based on the rule of mixture [86]. Here, the content of CNT used in the polymer matrix was 60 wt%. The absolute properties of the composites, especially mechanical properties were not as high as expected. This was attributed to poor CNT dispersion, impurity in the CNT and poor interfacial strength between the polymer and the CNT. However, a good-to-excellent tensile property composite can be obtained when high purity nanotubes are well dispersed and exfoliated in the polymer matrix [87–90]. It well known

that when a small quantity of carbon nanotube, particularly SWCNT, are dispersed and exfoliated in polymer matrix, the polymer orientation, and crystallization can be affected [91–97]. A faster crystallization rate occurs with the application of CNTs at higher temperatures. The study of isothermal crystallization of polyethylene/SWNT composites has shown that onset of crystallization can occur earlier in the composites than the neat polymer, and the crystallization rate is faster in the composite [98].

10.3.1.2 Dispersion and structural control of CNTs

Dispersion of CNTs is one of the major factors that strongly influence the properties of nanocomposites. These nanomaterials have a strong tendency to agglomerate due to the presence of attractive forces (Van der Waals), originating from their polarizable extended π-electron systems [99]. Infiltration of agglomerates with matrices is very difficult, thus their presence is the source of potential defects in nanocomposites. Factors responsible for dispersion are continuous detachment of small fragments at a comparatively lower stress level (erosion) and abrupt splitting up of agglomerates into small fragments under high stress (rupture). The dispersion behavior of CNF and CNT depends on a few critical factors, such as length of nanomaterials, their entanglement density, volume fraction, matrix viscosity, and attractive forces [99].

In the polymer nanocomposites CNTs are dispersed in the polymeric matrix [100]. The dispersion and arrangement of CNTs in the matrix (including their potential uniaxial alignment) hold central roles in controlling the properties of the resulting composites [83]. The inherent properties of CNT assume that the structure is well preserved, such as having large-aspect-ratio and no defects. Furthermore, the first step to the effective reinforcement of polymers using nanofillers is the achievement of a uniform dispersion of the fillers within the hosting matrix, and this is also related to the as-synthesized nanocarbon structure. Again, effective interfacial interaction and stress transfer between CNT and polymer is very important for improved mechanical properties of the fiber composite. Lastly, the excellent intrinsic mechanical properties of CNT similar to polymer molecules can be fully exploited only if an ideal uniaxial orientation is achieved [75]. Thus, during the fabrication of polymer/CNT fibers, four key areas need to be addressed and understood in order to successfully control the microstructural development in these composites. The key areas which are (i) CNT pristine structure, (ii) CNT dispersion, (iii) polymer-CNT interfacial interaction, (iv) orientation of the filler and matrix molecules is shown in Figure 10.4.

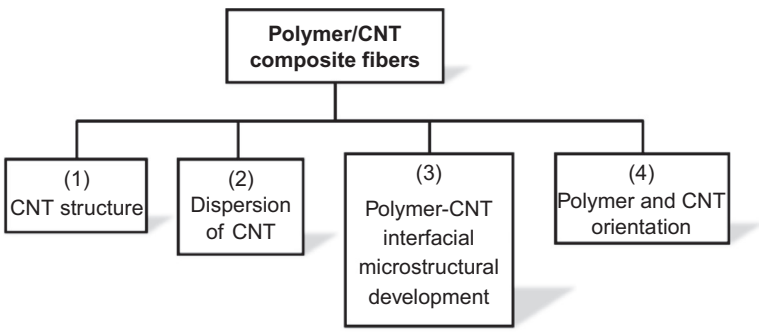

FIGURE 10.4

Four major factors affecting the microstructural development in polymer/CNT composite fiber during processing [75].

10.3.1.3 Methods of homogeneous dispersion of carbon nanomaterials

The common strategies to disperse CNTs fall into two general categories: chemical functionalization and noncovalent surface modification [101]. In order to achieve homogeneous dispersion of carbon nanomaterials in water and various polymers, different chemical methods have been used to date. The methods are use of solvents, surfactants, functionalization with acids, amines and the fluorines, plasma, microwave, and matrix moieties. Some researchers used noncovalent functionalization, block polymers, wrapping conjugated polymers, and other methods. Some of these methods will be discussed in this section.

Ausman et al. [102] performed a systematic study in order to find an appropriate medium for solubilization/dispersion of pristine SWCNTs. Five solvents, all featuring high electron pair donicity (â) and low hydrogen bond parameter (R) demonstrated the ability to readily form stable dispersions. To evaluate representative samples of each solvent category as determined by UV/visible spectroscopy, single drops of the centrifuged dispersions of SWCNT material in dimethylformamide (DMF), 4-chloroanisole, and toluene were dried overnight on glass microscope slides. These substrates were then imaged by noncontact atomic force microscopy (AFM). The DMF dispersion showed a high density of SWCNTs and ropes intertwined on the glass surface, confirming that the majority of the material dispersed was in fact nanotube material (see Figure 10.5).

Vaisman et al. [103] formed a uniform, multi-walled nanotubes (MWNTs) distribution in water-soluble (poly(ethylene glycol)) and water-insoluble (polypropylene) polymers. In order to understand the surface-charge-related stability of the treated nanotubes solutions, zeta-potential measurements were applied. Quantification of the state of the MWNT dispersion was derived from particle-size analysis, while visual characterization was based on optical and electron microscopy. In order to estimate the nucleating ability of the surface-modified CNTs, the temperature of crystallization and the degree of crystallinity were calculated from differential scanning thermograms.

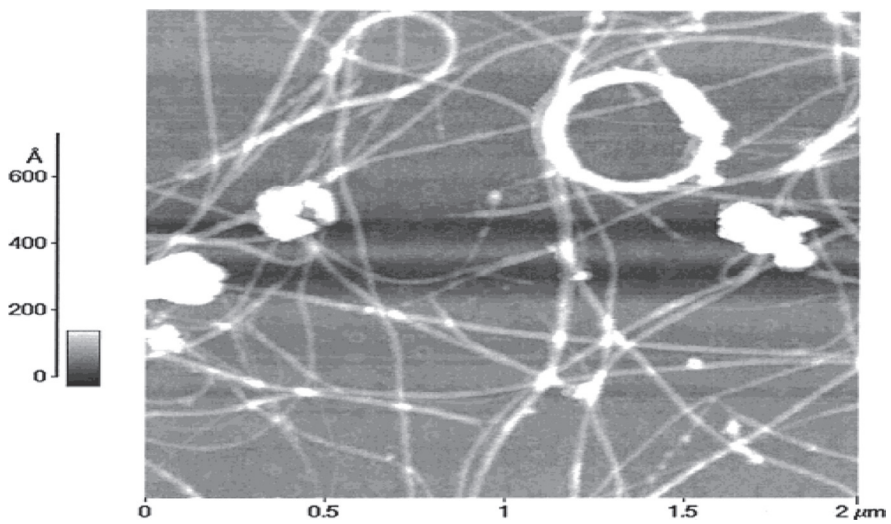

FIGURE 10.5

Noncontact AFM image of SWCNT material dispersed on a glass substrate from DMF dispersion [102].

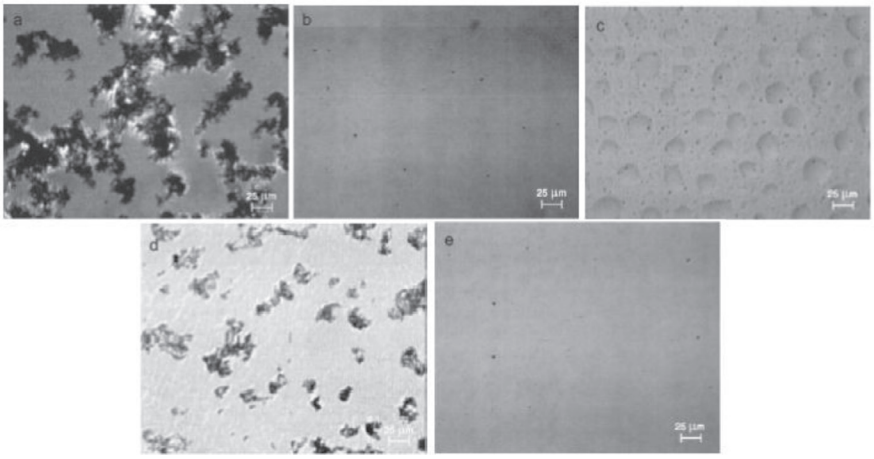

FIGURE 10.6

Optical microscope images of 1 wt% MWNT/PEG composite films. The CNT dispersion was governed by either surface modification via COOH functionalization, or by surfactant adsorption: (a) MWNT/PEG, (b) oxidized MWNT/PEG, (c) MWNT/PEG with Tween-80, (d) MWNT/PEG with Pluronic P-65, and (e) MWNT/PEG with DTAB [103].

The dispersive power of a wide range of surfactants was tested, in an attempt to improve the poor dispersion of pristine CNTs in a hydrophilic polyethylene glycol (PEG) solution shown in Figure 10.6a. Oxidized CNTs showed high-quality dispersion within the PEG matrix (see Figure 10.6b); this is due to a lowered tendency of the filler to aggregate, which can be attributed to the electrostatic repulsion effect. As shown in Figure 10.6c, tween-80 (poly(ethylene oxide) (20) sorbitan monooleate promotes the processing of highly homogenized MWNT/PEG composites. The incorporation of pluronic surfactants showed no improvement in CNT dispersion, and large, ~30 µm sized aggregates were formed (see Figure 10.6d). The insufficient block copolymer dispersive efficiency is probably associated with a bridging mechanism-long polymeric molecules of the surfactant adsorbed onto the surfaces of adjacent nanotubes, bridging them together, and creating a loose network. The findings shown in Figure 10.6e contradicted their expectations, and demonstrated a highly homogenized dodecyltrimethylammonium bromide (DTAB)-assisted dispersion of CNTs. According to the researchers [103], this phenomenon could be attributed to the adsorption of additional surfactant molecules by the interaction of their hydrophobic groups with those of previously adsorbed DTAB and with its hydrophilic groups oriented toward the PEG solution. Chen et al. [104] report the dispersion of MWCNTs using trifluoroacetic acid (TFA) as a cosolvent. Their study demonstrated that MWCNTs can be effectively purified and readily dispersed in a range of organic solvents including DMF, tetrahydrofuran (THF), and dichloromethane when mixed with 10 vol% TFA. The dispersed CNTs in TFA/THF solution were mixed with poly(methyl methacrylate) (PMMA) to fabricate polymer nanocomposites and a good dispersion of nanotubes in solution and in polymer matrices was observed and confirmed by scanning electron microscopy (SEM), optical microscopy, and light transmittance study (Figure 10.7). X-ray photoelectron spectroscopic analysis revealed that the chemical structure of the TFA-treated MWCNTs remained intact without oxidation. Few representative images of MWCNT/PMMA and MWCNT/P3HT/PMMA

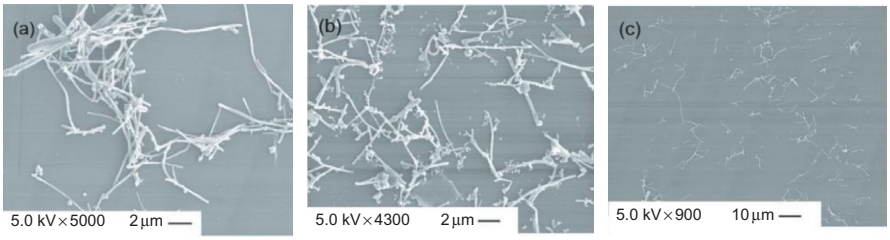

FIGURE 10.7

SEM images of type 1 MWCNTs suspended or dispersed in THF and then deposited on graphite substrates. (a) MWCNTs suspended in pure THF. (b) The as-obtained MWCNTs dispersed in 10 vol% TFA in THF. (c) MWCNTs after purification by multiple cycles of washing with 10 vol% TFA/DMF solvent and redispersed in 10 vol% TFA/THF solvent [104].

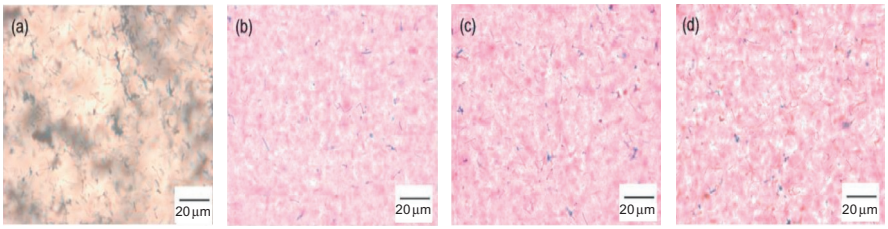

FIGURE 10.8

Optical images revealing the distribution of MWCNTs (aspect ratio: 100) in composite films. (a) MWCNT/PMMA film with 0.25 wt% of MWCNTs, (b–d) MWCNT/P3HT/PMMA film with (b) 0.07 wt%, (c) 0.13 wt%, and (d) 0.19 wt% of MWCNTs.

composite films with different loading ratios of MWCNTs are shown in Figure 10.8. Overall, CNTs are uniformly distributed through the polymer matrix at the loading ratios as shown. Two peaks were identified from X-ray photoelectron spectroscopy (XPS) spectrum of received MWCNTs (Figure 10.9a): a major peak at 284.7 eV, which is assigned to the conjugated C in CNTs, and a minor peak at 287.7 eV, which is attributed to impurity carbon in the form of C–OH. After purification of the MWCNTs by

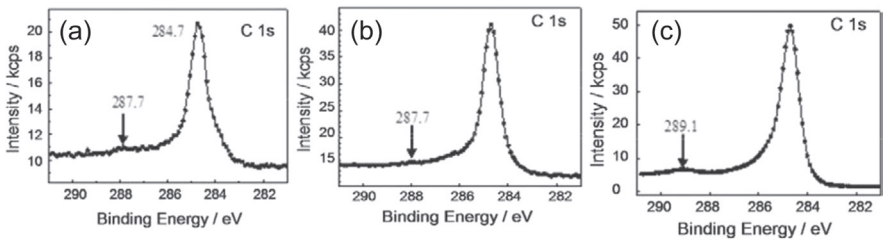

FIGURE 10.9

X-ray photoelectron spectra of (a) untreated MWCNTs, (b) MWCNTs treated by TFA, (c) MWCNTs treated by nitric acid [104].

mixed TFA/DMF solvent, the major peak at 284.7 eV remains the same, but the minor peak at 287.73 eV diminished almost completely (see Figure 10.9b). As a comparison, the XPS spectrum of nitric acid-treated MWCNTs is shown in Figure 10.9c. A peak corresponding to oxidized carbon at 289.1 eV in the form of COOH groups was clearly seen.

Mao et al. [105] recently reported noncovalent dispersion of CNTs in organic liquids with extremely high loading (2 mg mL^{-1}) using polyvinylferrocene (PVF). They showed that PVF can noncovalently disperse CNTs to individualized tubes with extremely high concentrations of organic solvents. They further demonstrated that PVF's redox-tunable affinity for organic solvents, together with its stable attachment to the nanotubes during redox transformation, allowed for controllable dispersion and aggregation of nanotubes. This opens up new avenues for tailoring CNT dispersion behavior via external stimuli, with potential applications in nanotube-based responsive systems, such as switching devices. This behavior further provides an electrochemically controlled approach to generating CNT-functionalized surfaces of different shapes, which can be used for sensing and catalysis. Noncovalent functionalization of nanotubes is of particular interest because it does not compromise the physical properties of CNTs, but improves solubility and processability [106].

10.3.2 RELATIONSHIP BETWEEN PREPARATION, STRUCTURE, AND PROPERTY OF POLYMER/GRAPHENE COMPOSITE MATERIALS

Graphenes show great promise as stronger, conductive fillers in polymer nanocomposites than CNTs; however, the persistent problem for graphene-based nanocomposites is the difficulty in achieving dispersion quality and interfacial strength between filler and matrix. Furthermore, attaining a large production volume of these materials is still challenging. Efforts have been made to develop high-quality graphene in large quantities for both research purposes and with a view to possible practical applications. Graphene can be prepared by the following methods: electrochemical exfoliation, chemical oxidation/exfoliation, and mechanical exfoliation followed by reduction of graphene derivatives such as graphene oxide (GO). Other methods are epitaxial growth on SiC and other substrates, chemical vapor deposition (CVD), chemical molecular assembly method, and arc discharging methods. All these methods have their advantages and disadvantages. Some of these methods will be discussed in this section. Both epitaxial growth and CVD techniques can also produce high-quality graphene with excellent physical properties. But, with these approaches, it is difficult to obtain a high enough yield to satisfy the need for its use as a composite filler [107]. At present, the most viable route to produce graphene in considerable quantities is reduction of graphite oxide. Graphite oxide is generally synthesized though oxidation of graphite using strong mineral acids and oxidizing agents [107].

10.3.2.1 Exfoliated graphite fillers

Exfoliation of graphite is a phase transition process that involves the vaporization of intercalate in the graphite. The exfoliation of graphite is a process in which graphite expands by up to hundreds of times along the c axis, resulting in a puffed-up material with a low density and a high temperature resistance [108]. Again, the compression of exfoliated graphite leads to a material with a high lubricity and flexibility. Exfoliated graphite could also be sued as fillers in composite even carbon fiber under appropriate conditions. However, the dispersion of graphene in common solvents is challenging due to the fact that exfoliation from graphite is inhibited by the strong, attractive Van der Waals forces holding the sheets together. Even after the initial process of exfoliation and dispersion, same attractive forces cause graphene to reaggregate.

Weak physical interactions (Van der Waals forces) are involved in the natural graphite, and material cohesion is possible only because of the very large number of interactions simultaneously acting among neighboring carbon sheets. Thus, the graphite structure is made of perfectly piled flat carbon sheets touching each other to allow induction of instantaneous dipoles among the neighbor carbon planes. Such a well-ordered structure is the basic condition for cohesion in graphite and the disordering of this piled structure significantly decreases the material cohesion [109]. Due to the high thermodynamically stable chemical structure, graphite is an inert substance, and only a few chemical reactions are possible using graphite as a reactant. Graphite flakes can be chemically modified by treatment with very strong oxidizing species leading to a chemical compound known as graphite oxide [56,110–112].

Chemically derived graphene is usually produced through oxidation graphite to graphite oxide with a hydrophilic layered structure. This is then exfoliated into the GO in aqueous media or polar solvents, possibly by mechanical shearing [113–115]. Due to the nature of the hydrophilic GO, it is not easily dispersed in weakly polar organic solvents, and polymers [116]. Reduction of GO always results in serve aggregation of the reduced GO (rGO) [73]. A lot of efforts have been made to disperse chemically derived graphene in low polarity organic media by functionalization of GO, but using aqueous dispersion of GO to fabricate graphene-based composite is more attractive. Aqueous dispersion of GO to fabricate graphene-based composite can be easily combined with water-soluble polymers and then reduced to rGO [117] without using organic solvents or chemical functionalization which can be toxic and/or costly [118,119]. Gudarzi and Sharif [120] proposed that by proper functionalization and mixing strategy of graphene, its dispersion, and bonding to the polymeric matrix can be improved. They applied this strategy to graphene-epoxy system by amino functionalization of GO (see Figure 10.10).

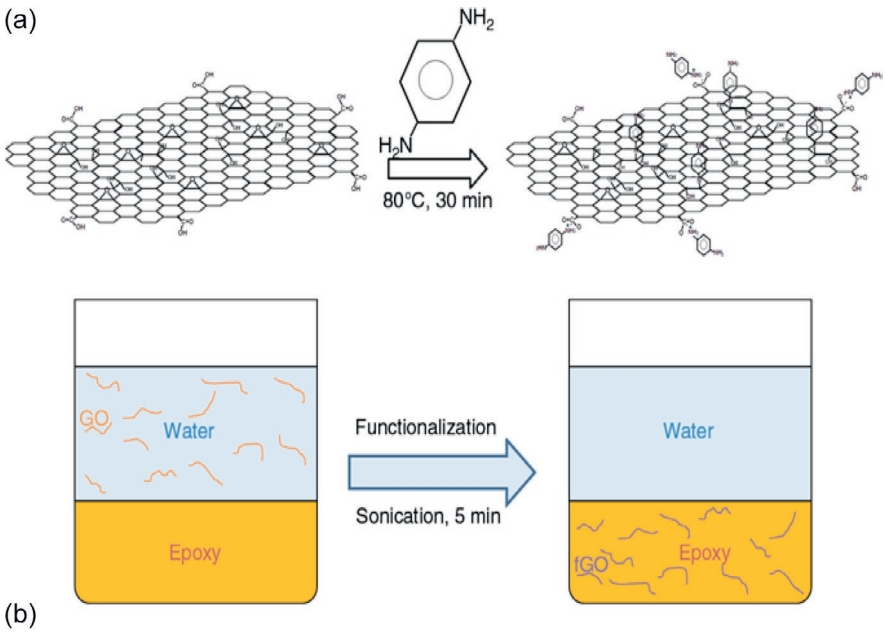

FIGURE 10.10

(a) Schematic representation of diamine bonding to GO. (b) Schematic illustration of transferring GO sheets from water to epoxy phase after functionalization [120].

The process included two phase extraction, and resulted in better dispersion and higher loading of graphene in epoxy matrix. Rheological evaluation of different graphene-epoxy dispersions showed a rheological percolation threshold of 0.2 vol% which was an indication of highly dispersed nanosheets (see Figure 10.11). As shown in Figure 10.12, the observation of the samples SEM showed dispersion homogeneity of the sheets at micro- and nanoscales. Study of graphene-epoxy composites showed good bonding between graphene and epoxy. Mechanical properties of the samples were consistent with theoretical predictions for ideal composites indicating molecular level dispersion and good bonding between nanosheets and epoxy matrix.

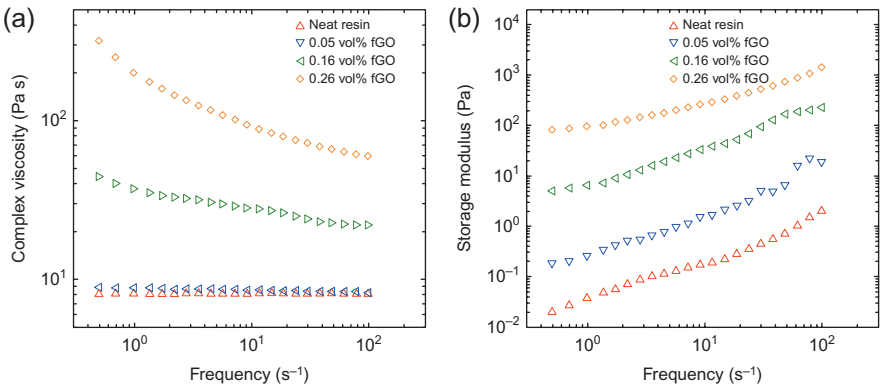

FIGURE 10.11

Results of rheometery for uncured epoxy-fGO mixtures with different fGO content (0-0.26 vol%) as a function of frequency at room temperature, (a) complex viscosity and (b) storage modulus [120].

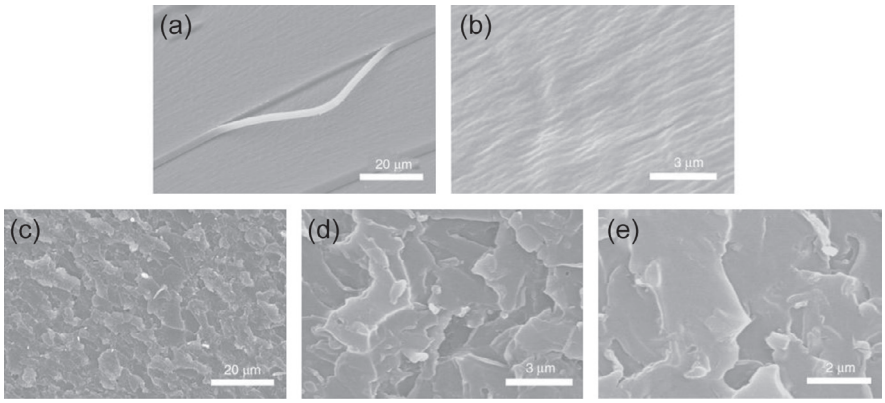

FIGURE 10.12

SEM images of fracture surface of (a, b) neat resin and (c–e) composite containing 0.2 vol% fGO at different magnifications [120].

Notarianni et al. [121] produced graphene by electrochemically exfoliating highly oriented pyrolytic graphite ($1 \times 1\,cm^2$) in a 150 mL aqueous solution containing 0.15 M Na_2SO_4 and 0.01 M sodium dodecyl sulfate. A Pt wire was used as a cathode and the voltage was set to be 5-6 V. The setup was placed in a sonicator during the electrochemical exfoliation process, which resulted in a final product consisting of mostly bilayer graphene. By using AFM to scan a number of graphene sheets randomly dispersed onto a mica substrate, statistics of the graphene flake thickness were obtained. They found that the thin graphene film with a thickness of <1 μm can greatly increase the capacitance. For composite applications, excellent dispersion is not enough; one must also have excellent interfacial adhesion for efficient stress transfer from the graphene to the polymer matrix.

10.3.2.2 Structure of exfoliated graphite

As explained in the previous section, graphene is a single layer of carbon atoms packed densely in a honeycomb crystal lattice. Exfoliated graphite exhibits a honeycomb microstructure because of the gas bubbles. The surface area of exfoliated graphite varies from one intercalate to another, e.g., nitric acid is an intercalate, which leads to a considerable bursting of the gas bubble, while bromine is an intercalate which does not burst. Thus, nitric acid yields exfoliated graphite with a much higher surface area than exfoliated graphite-bromine [108]. The carbon–carbon bond (sp^2) length in graphene is found to be approximately 0.142 nm [122,123]. The graphene layer thickness ranges from 0.35 to 1 nm relative to the SiO_2 substrate depending on the investigation [124].

The properties and structure of graphite oxide depend on the specific synthesis method and the degree of oxidation. Intercalation of graphite by a mixture of sulfuric and nitric acid produces a higher-stage GIC that can be exfoliated by the rapid heating or microwave treatment of the dried down powder, producing a material commonly referred to as expanded graphite (EG) [30]. EG retains a layered structure but has slightly increased interlayer spacing relative to graphite, consisting of thin platelets (30-80 nm), which are loosely stacked [30]. Lueking et al. [125] structurally characterized exfoliated graphite nanofibers (EGNFs) with transmission electron microscopy (TEM) and high-angle annular dark-field-scanning TEM (HAADF-STEM). Their investigation indicated that exfoliation has led to structural expansion along the fiber axis, with discrete domains of graphitic nanocones separated by gaps ranging from 50 to 500 Å (see Figure 10.13). Image contrast in HAADF-STEM demonstrated that structural expansion dominates over chemical etching (see Figure 10.14). Raman spectroscopy shown in Figure 10.15 indicated that the EGNF is more graphitic than the precursor, and the disappearance of the characteristic defect (*D*) peak with multi-wavelength excitation is inconsistent with the presence of amorphous carbon. The highly expanded EGNF structure oxidizes at two distinct rates at 750 °C in CO_2, leading to a highly disordered graphitic fiber, with apparent collapse of the expanded structure as no gaps or discrete graphitic domains are observed after oxidation. Variation in the heat input per intercalant mass during thermal shock leads to changes in fiber morphology, including the extent of fiber expansion, the number of defects and pores observable within the fiber via TEM, and the surface area measured by nitrogen adsorption [125].

After incorporation of graphite into polymer, the state of dispersion needs to be adequately determined in order to evaluate the reinforcement efficiency. Among various methods used for characterizing dispersion of layered nanocomposites, electron microscopy, and X-ray diffraction have been most widely used [126]. Imaging with TEM provides real space morphological information [125]. However, TEM only visualizes a small area. On the other hand, X-ray scattering yields structural information averaged over a larger sample volume.

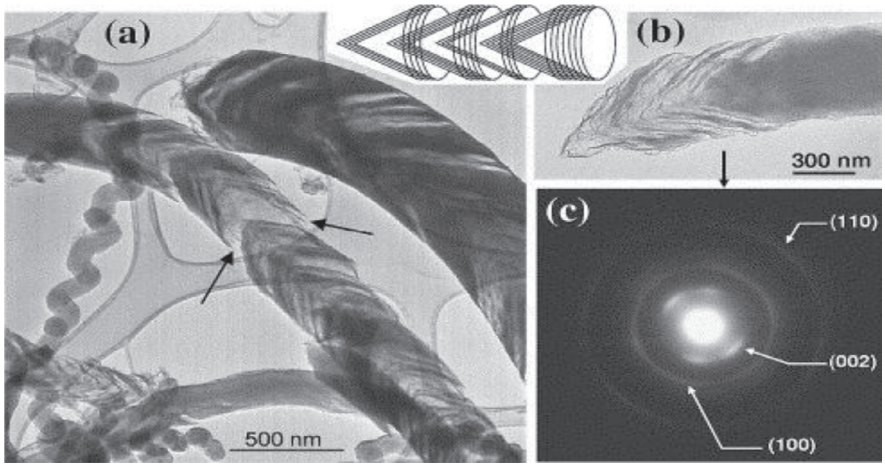

FIGURE 10.13

TEM analysis of EGNF-1000. Dark and light regions are observed in the fibers (a and b) after exfoliation. Certain fiber regions (arrows) with large expansion indicate fiber rupture. (c) SAED pattern of the nanofiber in (b), (002), (100), and (110) diffraction planes can be observed. The inset is a schematic model of the cup-stacked crystalline structure of the fiber after exfoliation; those segments of the fiber keeping the graphite spacing between cups (~3.35 Å) are responsible for the (002) diffraction spots observed in the SAED pattern [125].

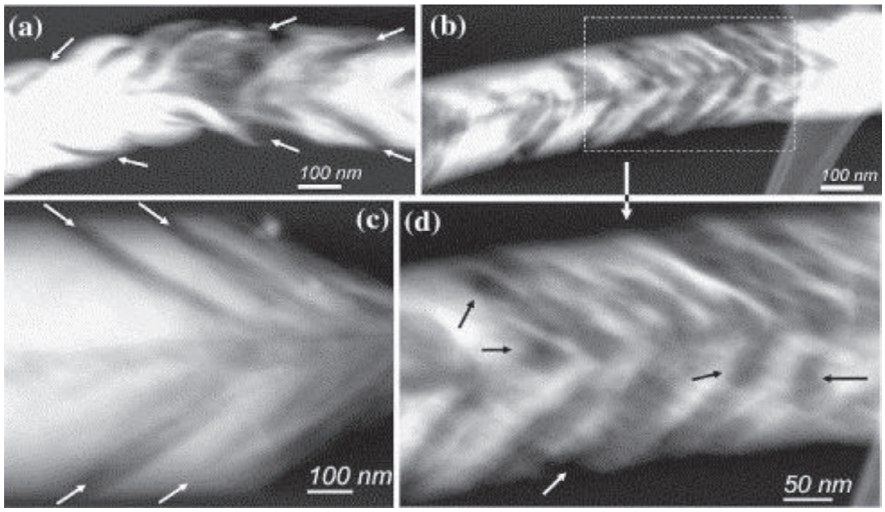

FIGURE 10.14

HAADF-STEM of EGNF-1000: (a–c) are different examples of individual fibers. (d) Higher magnification of (b). Straight gaps (dark contrast) symmetrically distributed around the fiber axis (center) suggest expansion (arrows in (a) and (b)) and gaps with asymmetric shapes suggest chemical etching (arrows in (d)). The appearance of bands in HAADF-STEM imaging is inconsistent with the presence of amorphous carbon [125].

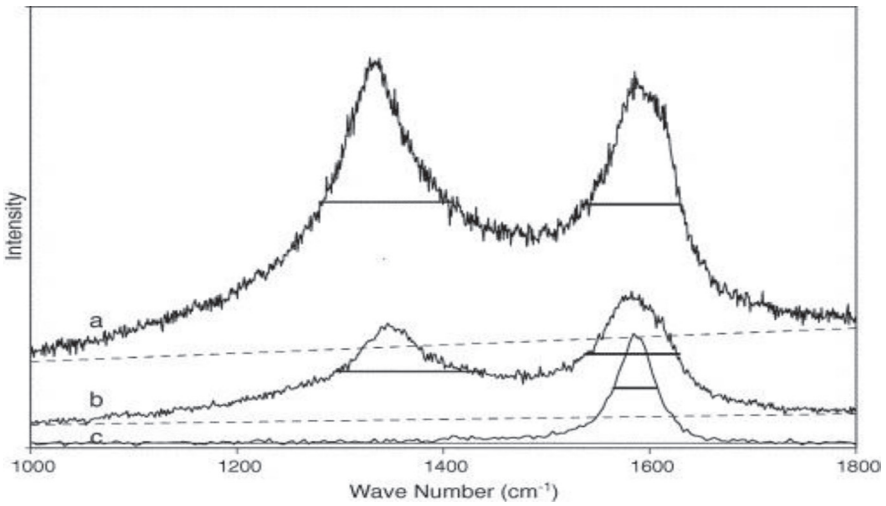

FIGURE 10.15

Multi-wavelength Raman of EGNF-1000 with excitation wavelength of (a) 633 nm, (b) 514 nm, and (c) 257 nm. Horizontal bars denote full-width half-maxima for the peaks, and the dotted line is drawn to guide the eye for the background fit that was used in the calculation of the peak intensity [125].

10.4 GRAPHENATED CNTs

Graphenated CNTs are relatively new nanostructures in the carbon nanomaterial family that combines graphitic foliates grown along sidewalls of MWCNTs or bamboo style CNTs. Different methods are available for the preparation of graphene-CNT hybrid; two simple methods that are often used are: (1) preparation of GO-CNT hybrid by ultrasonication of GO and CNT mixture, and (2) subsequent reduction of GO-CNT hybrid to graphene with some specific post treatments [127–129]. Yen et al. [130] reported a two-step solution-based method at room temperature for the preparation of graphene-MWCNT hybrid material comprising graphene and acid-treated MWCNT (see Figure 10.16). The preparation methods involve synthesis of GO from graphite by Staudenmaier's method and consequent thermal reduction to graphene at 1050 °C followed by mixing of graphene with acid-treated MWCNTs and ultrasonication to get the final hybrid. A noncovalent π-π stacking interaction operating between graphene sheets and CNTs were revealed, which help to avoid the aggregation of individual graphene sheets.

Quite a number of exciting properties and applications of this novel carbon material have been reported in the literature [131,132]. Yu et al. [133] did some investigation on chemically bonded leaves growing alongside walls of CNT. They reported on a brand-new, three-dimensional carbon nanostructure comprising few-layer graphene (FLG) sheets inherently connected with CNTs through sp^2 carbons, resembling plant leaves (FLGs) growing on stems (CNTs). The evolution of FLG sheets on CNTs was tracked by high-resolution TEM (see Figure 10.17). Distinct from a random mixture of CNTs and graphene sheets (CNT + G) suffering from poor CNT-graphene contacts, their CNT-FLG structure has intrinsic chemical bonding between the two constituent components. They further showed that the resulting CNT-FLG structure exhibits remarkable optoelectronic and gas-sensing properties superior to its CNT or CNT + G counterparts.

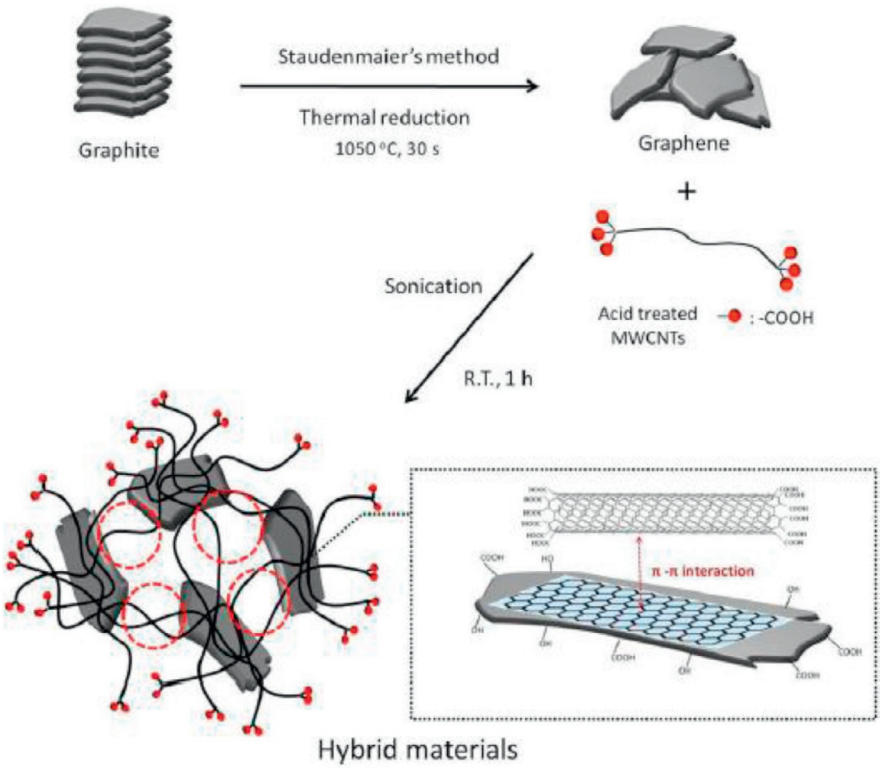

FIGURE 10.16

The schematic diagram representing the mechanism for the preparation of graphene-CNT hybrid material [130].

Tian et al. [134] provided simultaneous growth of graphene and SWCNTs, leading to the formation of three-dimensional interconnected networks. They also brought the intrinsic dispersion of graphene and CNTs and the dispersion of N-containing functional groups within a highly conductive scaffold. Their hybrid material presented high catalytic activity towards oxygen evolution reaction, rendering them high-performance heap catalysts for both oxygen reduction reaction and oxygen evolution reaction. Wimalasiri and Zou [135] combined SWCNTs with GO nanosheets in aqueous dispersion and then chemically reduced it to form the carbon nanotube/graphene (CNT/G) composite as electrodes for capacitive deionization (CDI). The structure of the CNT/G composite was highly porous, with SWCNTs sandwiched between graphene sheets that functioned as spacers and provided diffusion paths for smooth and rapid ion conduction. The associated increase in the electrical double-layer capacitance enhanced CDI performance. Pham et al. [136] reported the direct growth of a unique all-carbon hierarchical graphene-carbon nanotube (G-CNT) hybrid structure on Toray carbon paper using CVD methods. The morphological characterization in Figure 10.18 shows that the graphene was directly grafted onto the CNT scaffold. The hybrid possesses an ultra-high density of exposed graphene edges while retaining the porous structure of CNT scaffold. Using the G-CNT hybrid in the magnetron sputtering

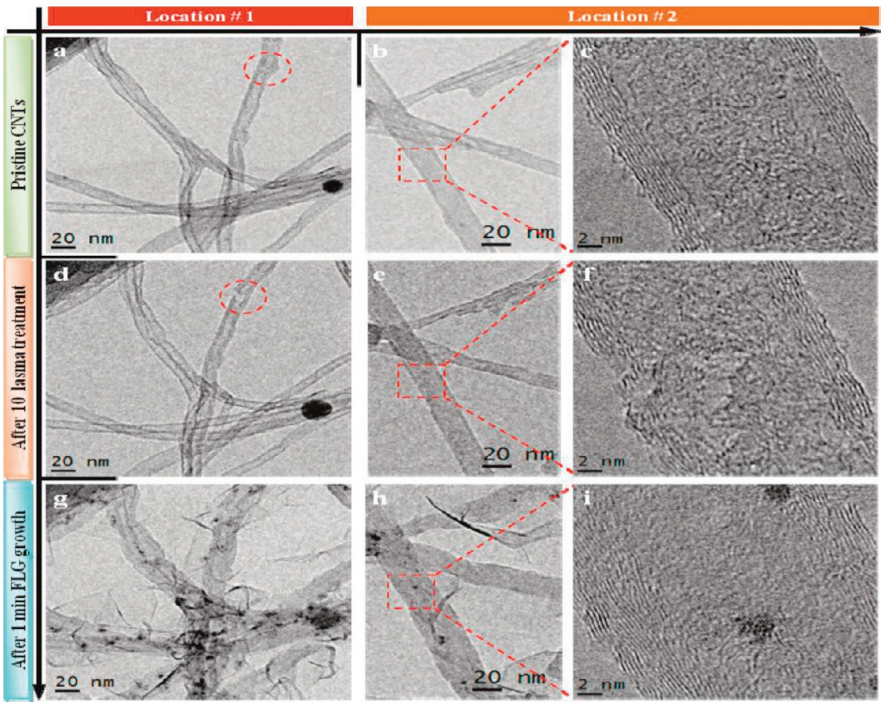

FIGURE 10.17

TEM and HRTEM (right column) images from two locations (Location 1: left column; Location 2: middle and right columns) in Sample A. (a–c) Pristine CNTs, (d–f) CNTs after being treated in Ar plasma for 10 s, (g–i) CNTs after a subsequent PECVD process for 1 min FLG growth [133].

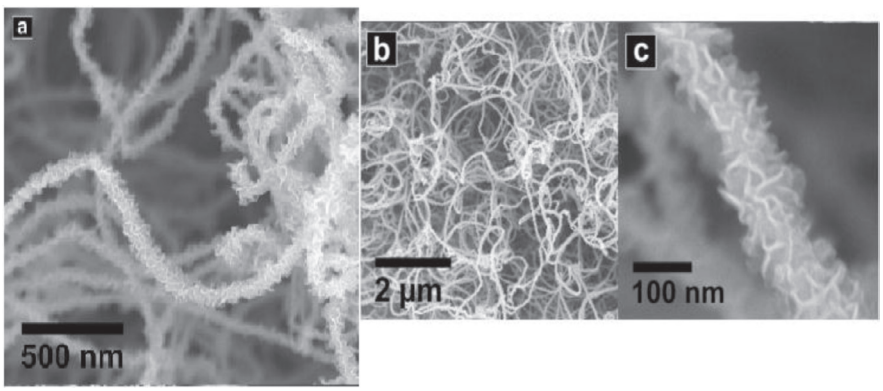

FIGURE 10.18

Morphological characterization of the G-CNT hybrid on carbon paper. SEM micrographs of the hybrid at (a) medium magnification, (b) lower magnification, and (c) higher magnification [136].

electrocatalyst preparation technique, an integrated, polytetrafluoroethylene binder-free cathode (Pt/G-CNT) with an ultra-low Pt loading of 0.04 mg cm^{-2} was obtained. This cathode showed superior polarization performance compared to a commercial carbon black-supported Pt catalyst.

The advantage of integrating graphene to CNTs structure is the high surface area three-dimensional framework of the CNTs coupled with the high edge density of graphene. The nature of graphene edges determines the structural properties of the material of interest. Graphene edges determine the optical, magnetic, electrical, and electronic properties of graphene [137]. Graphene edges provide significantly higher charge density and reactivity than the basal plane, but they are difficult to arrange in three-dimensional, high-volume-density geometry. CNTs are readily aligned in high-density geometry, but lack high-charge-density surfaces. The sidewalls of the CNTs are similar to the basal plane of graphene and exhibit low-charge density except where edge defects exit [138]. When compared to another carbon nanostructure, the deposition of a high density of graphene foliates along the length of aligned CNTs cab greatly increases the total charge capacity unit of nominal areas [139].

10.5 CURRENT APPLICATIONS OF CNTs AND GRAPHENE

CNTs, graphene and their compounds possess exceptional electrical properties for organic materials, and they have a huge potential in electrical and electronic applications, such as photovoltaics, sensors, semiconductor devices, display devices, conductors, smart textiles, and energy conversion devices (e.g., fuel cells, harvesters, and batteries). CNTs and graphene can greatly contribute to sustainable energy supplies and they are widely used in biomedicine.

Seo et al. [140] recently reported the growth of high-quality GaN layer on SWCNTs and graphene hybrid structure (CGH) as an intermediate layer between GaN and sapphire substrate by metal-organic chemical vapor deposition (MOCVD) and fabrication of light-emitting diodes (LEDs) using them. The SWCNTs on graphene act as nucleation seeds, resulting in the formation of kink bonds along SWCNTs with the basal plane of the substrate. The high crystalline quality of GaN layers grown on CGH/sapphire was observed to be due to the reduced threading dislocation and efficient relaxation of residual compressive strain caused by lateral overgrowth process. When applied to the LED structure, the current-voltage characteristics and electroluminescence (EL) performance exhibit that blue LEDs fabricated on CGH/sapphire well-operate at high injection currents and uniformly emit over the whole emission area. We expect that CGH can be applied for the epitaxial growth of GaN on various substrates such as Si and MgO, which can be a great advantage in electrical and thermal properties of optical devices fabricated on them.

Dye-sensitized solar cells (DSSCs) are prominent photovoltaic technology with both low costs and good efficiency. The cathode used in most DSSCs is fluorine-doped tin oxide glass coated with a Pt film, which is both expensive and brittle and thus limits the flexibility and large-scale implementation of this positive technology. Dong et al. [141] recently showed that flexible, seamlessly covalently bonded, three-dimensional vertically aligned few-walled CNTs (VAFWCNTs)/graphene on metal foil can act as a novel cathode free from transparent conducting oxide and Pt for application in DSSCs. This cathode has a lower charge transfer resistance and lower contact resistance between the catalyst and the substrate than the conventional combination in a brittle Pt/fluorine-doped tin oxide cathode. The covalently bonded graphene and VAFWCNTs ensure excellent electron transport through the

electrode and the large surface area of the hybrid carbon materials rivals the catalytic capability of the Pt analogue. The combination of VAFWCNTs/graphene on metal foil is a novel, inexpensive, high-performance, flexible cathode for application in solar cells. Pham et al. [136] also recently reported the direct growth of a unique all-carbon hierarchical G-CNT hybrid structure as catalyst support for high-performance proton exchange membrane (PEM) fuel cells on Toray carbon paper using CVD methods.

A wide range of materials such as graphene and other carbon nanocompounds which have different physical and chemical properties can be expected to react differently upon contact with biomolecules, cells, and tissues [142]. CNTs and graphenes have shown great promise for advancing the fields of biology and medicine. Fan et al. [143] reported a green and facile procedure of synthesizing a graphene nanosheet-carbon nanotube-iron oxide nanoparticle hybrid (GN–CNT–Fe_3O_4) as a promising platform for the loading and delivery of anticancer drugs. The obtained GN–CNT–Fe_3O_4 hybrid exhibited super paramagnetic properties with the saturation magnetization of 19.824 emu g^{-1}. This hybrid nanostructure possesses the superior capability of binding the anticancer drug 5-fluorouracil (5-FU) with a high loading capacity of up to 0.27 mg mL^{-1} with a 5-FU concentration of 0.5 mg mL^{-1}, and also possesses a pH-activated release profile. Their studies show that the resulting GN–CNT–Fe_3O_4 hybrid can be internalized efficiently by HepG2 cells. *In vitro* cytotoxicity tests suggested that the obtained GN–CNT–Fe_3O_4 hybrid was nontoxic for Chang liver cells, even at the high concentration of 80 μg mL^{-1}; however, the 5-FU-loaded GN–CNT–Fe_3O_4 hybrid showed significant cytotoxic effects in HepG2 cells. The results showed that the novel three-dimensional hybrid is a promising candidate for anticancer drug-delivery systems.

10.6 CONCLUSION

The discussion of nanotechnology perspectives in this chapter is centered on carbon-based nanostructures (CNTs and graphenes). To a considerable degree, the popularity of carbon nanostructures is due to fullerenes and nanotubes, other members of the carbon family are also steadily gaining attention. Diamond, graphite, tubes, and newly discovered graphene are the most studied allotropes of the carbon family. Due to the chemical inertness of graphitic walls, functionalization of CNTs, and graphene is usually the key step required in the applications of these materials. For a successful CNT/composite development, good mechanical properties must be achieved in a cost-effective manner and CNTs must then be processed in such a way as to ensure that a homogeneous dispersion is obtained within the matrix, whilst developing an appropriate degree of interfacial bonding. The dispersion of nanomaterials in polymeric matrices also plays an important role in determining the final properties of the composite materials.

Graphene has recently attracted considerable scientific interest because of its unique mechanical, electrical, and thermal properties which may enable a range of advanced materials and devices including nanocomposites thin conductive films. Dispersion of graphene in nano scale, and especially in single layers, provides the best opportunity for bonding.

The relationship between preparation, structure, and property of polymer/graphene composite materials is discussed in this chapter. Some graphenated CNTs were also discussed. Some recent advances on graphene CNTs hybrid were discussed.

10.7 RECOMMENDATION

Advances in computational materials science in general will continue to facilitate the understanding of CNTs and graphene materials together with their processing. Therefore, the prediction of properties, materials behavior and the design of these new materials and phases will facilitate the application of science and engineering to developing more sophisticated and innovative processes.

The complex interactions in polymer composites influence the nanostructure formation, thereby influencing their properties. It is also known that the properties of the nanostructured polymer composites can be tailored through control of various molecular interactions. Many parameters need to be well controlled in order to develop high-quality materials; thus, multiscale molecular modeling can be successfully applied in process system applications in science and engineering for the estimation of the properties of pure components and mixtures of CNT and graphene, in order to successfully control the properties and interaction parameters of the nanostructured materials. In the polymer nanocomposites, CNTs, and graphenes are dispersed in the polymeric matrix, therefore homogeneous dispersion of these carbon nanomaterials in water and various polymers can also be successfully achieved with the use of molecular modeling.

REFERENCES

[1] Inagaki M, Radovic LR. Nanocarbons. Carbon 2002;40:2279–82.
[2] Inagaki M, Kaneko K, Nishizawa T. Nanocarbons-recent research in Japan. Carbon 2004;42:1401–7.
[3] Shahriary L, Ghourchain H, Athawale AA. Graphene-multiwalled carbon nanotube hybrids synthesized by gamma radiations: application as a glucose sensor. J Nanotechnol 2014;903872:1–10.
[4] Bael S, Kim SJ, Shin D, Ahn JH, Hong BH. Towards industrial applications of graphene electrodes. Phys Scr 2012;T146:1–8.
[5] Dharap P, Li Z, Nagarajaiah S, Barrera EV. Flexural strain sensing using carbon nanotube film. Sensor Rev 2004;24(3):271–3.
[6] Saha D, Li Y, Bi Z, Chen J, Keum JK, Hensley DK, et al. Studies on supercapacitor electrode material from activated lignin derived mesoporous carbon. Langmuir 2014;30(3):900–10.
[7] Zheng G, Lee SW, Liang Z, Lee H-W, Yan K, Yao H, et al. Interconnected hollow carbon nanospheres for stable lithium metal anodes. Nat Nanotechnol 2014;9:618–23.
[8] Zhang W, Silva SRP. Application of carbon nanotube in polymer electrolyte based on fuel cell. Rev Adv Mater Sci 2011;29:1–14.
[9] Liu F, Piao Y, Choi KS, Seo TS. Fabrication of free-standing graphene composite films as electrochemical biosensors. Carbon 2012;50(1):123–33.
[10] Papaginnouli I, Bourlinos AB, Bakandritsos A, Couris S. Nonlinear optical properties of colloidal carbon nanoparticles: nanodiamonds and carbon dots. RSC Adv 2014;4(76):40152–60.
[11] Arash B, Wang Q, Varadan VK. Mechanical properties of carbon nanotube/polymer composites. Sci Rep 2014;4:1–8.
[12] Balandi AA. Thermal properties of graphene and nanostructured carbon materials. Nat Mater 2011;10:569–81.
[13] Makarova TL. Magnetic properties of carbon structures. Semiconductors 2004;38(6):615–38.
[14] Bandaru PR. Electrical properties and applications of carbon nanotube structures. J Nanosci Nanotechnol 2007;7:1–29.
[15] Ganesh EN. Single walled and multi walled carbon nanotube structure, synthesis and applications. Int J Innov Technol Explor Eng 2013;2(4):311–20.

[16] Breuer O, Sundararaj U. Big returns from small fibers: a review of polymer/carbon nanotube composites. Polym Compos 2004;25:630–41.
[17] Cirillo G, Hampel S, Spizzirri UG, Parisi OI, Picci N, Iemma F. Carbon nanotubes hybrid hydrogels in drug delivery: a perspective review. Biomed Res Int 2014;825017:1–17.
[18] Vul AY, Shenderova OA. Detonation nano diamond science and applications. USA: CRC Press, Taylor and Francis Group; 2014, p. 4.
[19] Zhou YS. Laser-assisted nanofabrication of carbon nanostructures. Austin J Nanomed Nanotechnol 2014;2(2):1–18.
[20] Kuchibhatla SVNT, Karakoti AS, Bera D, Seal S. One dimensional nanostructured materials. Prog Mater Sci 2007;52:699–913.
[21] Dresselhaus MS, Dresselhaus G, Saito R. Nanotechnology in carbon materials. In: Timp G, editor. Nanotechnology. AIP Press; Springer, New York 1999. p. 285–331.
[22] Shenderova OA, Zhirnov VV, Brenner DW. Carbon nanostructures. Crit Rev Solid State Mater Sci 2002;27(3/4):227–356.
[23] Stone BR, Glass JT. Carbon nanostructures: a morphological classification for charge density optimization. Diam Relat Mater 2012;23:130–4.
[24] Penumadu D, Dutta A, Pharr GM, Files B. Mechanical properties of blended single wall carbon nanotube composites. J Mater Res 2003;18(8):1–3.
[25] Kumar S, Dang TD, Arnold FE, Bhattacharyya AR, Min BG, Zhang X, et al. Synthesis, structure, and properties of PBO/SWNT composites. Macromolecules 2002;35:9039–43.
[26] Ando T. The electronic properties of graphene and carbon nanotubes. NPG Asia Mater 2009;1(1):17–21.
[27] Chieng BW, Ibrahim NA, Zin WM, Yunus W, Hussein MZ. Poly(lactic acid)/poly(ethylene glycol) polymer nanocomposites: effects of graphene nanoplatelets. Polymer 2014;6:93–104.
[28] Das TK, Prusty M. Graphene-based polymer composites and their applications. Polym Plast Technol Eng 2013;52:319–31.
[29] Du J, Zhao L, Zeng Y, Zhang L, Li F, Liu P, et al. Comparison of electrical properties between multi-walled carbon nanotube and graphene nanosheet/high density polyethylene composites with a segregated network structure. Carbon 2011;49:1094–100.
[30] Potts JR, Dreyer DR, Bielawski CW, Rouf RS. Graphene-based polymer nanocomposites. Polymer 2011;52:5–25.
[31] Lee YR, Raghu AV, Jeong HM, Kim BK. Properties of waterborne polyurethane/functionalized graphene sheet nanocomposites prepared by an in situ method. Macromol Chem Phys 2009;210:1247–54.
[32] Li Q, Kim JW, Shim TH, Jang YK, Lee JH. Positive temperature coefficient behaviour of the graphite nanofibre and carbon black filled high-density polyethylene hybrid composites. Adv Mater Res 2008;47:226–9.
[33] Wang H, Zhang H, Zhao W, Zhang W, Chen G. Preparation of polymer/oriented graphite nanosheet composite by electric field inducement. Compos Sci Technol 2008;68:238–43.
[34] Chen X, Zheng YP, Kang F, Shen WC. Preparation and structure analysis of carbon/carbon composite made from phenolic resin impregnation into exfoliated graphite. J Phys Chem Solids 2006;67:1141–4.
[35] Rath D, Chahataray R, Nayak PL. Synthesis and characterization of conducting polymers multi walled carbon nanotube-chitosan composites coupled with poly (metachloroniline). Middle-East J Sci Res 2013;18(5):635–41.
[36] Chipara M, Cruz J, Vega ER, Alarcon J, Mion T, Chipara DM, et al. Polyvinylchloride-single-walled carbon nanotube composites: thermal and spectroscopic properties. J Nanomater 2012;435412:1–6.
[37] Mazinani S, Ajji A, Dubois C. Morphology, structure and properties of conductive PS/CNT nanocomposite electrospun mat. Polymer 2009;50:3329–42.
[38] Geng Y, Liu MY, Li J, Shi XM, Kim JK. Effects of surfactant treatment on mechanical and electrical properties of CNT/epoxy nanocomposites. Compos Part A 2008;39:1876–83.

[39] Kashiwagi T, Fagan J, Douglas JF, Yamamoto K. Relationship between dispersion metric of PMMA/SWNT nanocomposites. Polymer 2007;48(16):4855–66.
[40] Hoover LA, Schiffman JD, Elimelech M. Nanofibers in thin-film composite membrane support layers: enabling expanded application of forward and pressure retarded osmosis. Desalination 2013;308:73–81.
[41] Khanna V, Bakshi BR. Carbon nanofiber polymer composites: evaluation of life cycle energy use. Environ Sci Technol 2009;43:2078–84.
[42] Chipara M, Lozano K, Hernandez A, Chipara M. TGA analysis of polypropylene-carbon nanofibers composites. Polym Degrad Stab 2008;93:871–6.
[43] Tibbetts GG, Lake ML, Strong K, Rice BP. A review of the fabrication and properties of vapor-grown carbon nanofiber/polymer composites. Compos Sci Technol 2007;67:1709–18.
[44] Ichkitidze L, Podgaetsky V, Selishchev S, Blagov E, Galperin V, Shaman Y, et al. Electrically-conductive composite nanomaterial with multi-walled carbon nanotubes. Mater Sci Appl 2013;4:1–7.
[45] Shang SM, Zeng W, Tao XM. Highly stretchable conductive polymer composited with carbon nanotubes and nanospheres. Adv Mater Res 2010;123:109–12.
[46] Spitalsky Z, Tasis D, Papagelis K, Galiotis C. Carbon nanotube-polymer composites: chemistry, processing, mechanical and electrical properties. Prog Polym Sci 2010;35:357–401.
[47] Jeevananda T, Kim NH, Lee JH, Siddaramaiah B, Deepa Urs MV, Ranganathaiah C. Investigation of multi-walled carbon nanotube reinforced high-density polyethylene/carbon black nanocomposites using electrical DSC and positron lifetime spectroscopy techniques. Polym Int 2009;58:755–80.
[48] Liu N, Luo F, Wu H, Liu Y, Zhang C, Chen J. One step ionic-liquid assisted electrochemical synthesis of ionic-liquid-functionalized graphene sheets directly from graphene. Adv Funct Mater 2008;18:1518–25.
[49] Gupta A, Choudhary V. Electromagnetic interference shielding behaviour of poly [trimethylene terephthalate]/multi-walled carbon nanotube composites. Compos Sci Technol 2011;71:1563–8.
[50] Sohi NJS, Rahaman M, Khastgir D. Dielectric property and electromagnetic interference shielding effectiveness of ethylene vinyl acetate-based conductive composites: effect of different type of carbon fillers. Polym Compos 2011;32:1148–54.
[51] Lee JH, Kim SK, Kim NH. Effects of the addition of multi-walled carbon nanotubes on the positive temperature coefficient characteristics of carbon black- filled high-density polyethylene nanocomposites. Scr Mater 2006;55:1119–22.
[52] Sun Y, Bao HD, Guo ZX, Yu J. Modeling of the electrical percolation of mixed carbon fillers in polymer-based composites. Macromolecules 2009;42:459–63.
[53] Liu C-X, Choi J-W. Improved dispersion of carbon nanotubes in polymers at high concentrations. Nanomaterials 2012;2:329–47.
[54] Park SH, Theilmann P, Yang K, Rao AM, Bandaru PR. The influence of coiled nanostructure on the enhancement of dielectric constants and electromagnetic shielding efficiency in polymer composites. Appl Phys Lett 2011;96:043115.
[55] Kuilla T, Bhadra S, Yao D, Kim NH, Bose S, Lee JH. Recent advances in graphene based polymer composites. Prog Polym Sci 2010;35:1350–75.
[56] Dreyer RD, Park S, Bielawski CW, Ruoff RS. The chemistry of graphene oxide. Chem Soc Rev 2010;39:228–40.
[57] Wang G, Shen X, Wang B, Yao J, Park J. Synthesis and characterization of hydrophilic and organophilic graphene nanosheets. Carbon 2009;47:1359–64.
[58] Li X, Wang X, Zhang L, Lee S, Dai H. Chemically derived, ultra smooth graphene nanoribbon semiconductor. Science 2008;319:1229–31.
[59] Lianga J, Wanga Y, Huang Y, Maa Y, Liua Z, Caib J, et al. Electromagnetic interference shielding of graphene/epoxy composites. Carbon 2009;47:922–5.
[60] Vovchenko LL, Matzui LY, Oliynyk VV, Launetz VL. The effect of filler morphology and distribution on electrical and shielding properties of graphite-epoxy composites. Mol Cryst Liq Cryst 2011;535:179–88.

[61] Bourlinos AB, Georgakilas V, Zboril R, Steriotis TA, Stubos AK, Trapalis C. Aqueous-phase exfoliation of graphite in the presence of polyvinylpyrrolidone for the production of water-soluble graphenes. Solid State Commun 2009;149:2172–6.
[62] Kim H, Macosko CW. Morphology and properties of polyester/exfoliated graphite nanocomposites. Macromolecules 2008;41:3317–27.
[63] Song P, Cao Z, Cai Y, Zhao L, Fang Z, Fu S. Fabrication of exfoliated graphene-based polypropylene nanocomposites with enhanced mechanical and thermal properties. Polymer 2011;52:4001–10.
[64] Quan H, Zhang B, Zhao Q, Yuen RKK, Li RKY. Facile preparation and thermal degradation studies of graphite nanoplatelets (GNPs) filled thermoplastic polyurethane (TPU) nanocomposites. Compos Part A 2009;40:1506–13.
[65] Eda G, Chhowalla M. Graphene-based composite thin films for electronics. Nano Lett 2009;9:814–8.
[66] Zhao S, Zhang Q, Chen D. Enhanced mechanical properties of graphene-based poly(vinyl alcohol) composites. Macromolecules 2010;43(5):2357–63.
[67] Naebe M, Wang J, Amini A, Khayyam H, Hameed N, Li LH, et al. Mechanical property and structure of covalent functionalised graphene/epoxy nanocomposites. Sci Rep 2014;4(4375):1–7.
[68] Yoo BM, Shin HJ, Yoon HW, Park HB. Graphene and graphene oxide and their uses in barrier polymers. Appl Polym 2014;131(1):39628–750.
[69] Yang J, Bai L, Feng G, Yang X, Lv M, Zhang C, et al. Thermal reduced graphene based poly(ethylene vinyl alcohol) nanocomposites: enhanced mechanical properties, gas barrier, water resistance, and thermal stability. Ind Eng Chem Res 2013;52(47):16745–54.
[70] Shen M-Y, Kuan C-F, Kuan H-C, Chen C-H, Wang J-H, Yip M-C, et al. Preparation, characterization, thermal, and flame-retardant properties of green silicon-containing epoxy/functionalized graphene nanosheets composites. J Nanomater 2013;747963:1–10.
[71] Liang J, Xu Y, Huang Y, Zhang L, Wang Y, Ma Y, et al. Infrared triggered actuators from graphene-based nanocomposites. J Phys Chem 2009;113:9921–7.
[72] Kim H, Macosko CW. Processing-property relationships of polycarbonate/graphene nanocomposites. Polymer 2009;50:3797–809.
[73] Stankovich S, Dikin DA, Dommett GHB, Kohlhaas KM, Zimney EJ, Stach EA, et al. Graphene-based composite materials. Nature 2006;442:282–6.
[74] Njuguna J. Structural nanocomposite: perspectives for future application. United Kingdom: Springer-Verlag Berlin Heidelberg; 2013, p. 20.
[75] Song K, Zhang Y, Meng J, Green EC, Tajaddod N, Li H, et al. Structural polymer-based carbon nanotube composite fibers: understanding the processing–structure–performance relationship. Materials 2013;6:2543–77.
[76] Lewandowski Z, Ziabicki A, Jarecki L. The nonwovens formation in the melt-blown process. Fibres Text East Eur 2007;15(50):64–5.
[77] Jia J. Melt spinning of continuous filaments by cold air attenuation. Thesis, Doctor of Philosophy. Georgia Institute of Technology; 2010.
[78] Benavides RE, Jana SC, Reneker DH. Nanofibers from scalable gas jet process. ACS Macro Lett 2012;1:1032–6.
[79] Ziabicki A. Fundamentals of fibre formation: the science of fibre spinning and drawing. John Wiley & Sons, Ltd; New York 1976.
[80] Lemstra PJ, Bastiaansen CWM, Meijer HEH. Chain-extended flexible polymers. Angew Makromol Chem 1986;145:343–58.
[81] Wang T, Kumar S. Electrospinning of polyacrylonitrile nanofibers. J Appl Polym Sci 2006;102:1023–9.
[82] Huang ZM, Zhang YZ, Kotaki M, Ramakrishna S. A review on polymer nanofibers by electro-spinning and their applications in nanocomposites. Compos Sci Technol 2003;63:2223–53.

[83] Huang YY, Terentjev EM. Dispersion of carbon nanotubes: mixing, sonication, stabilization and composite properties. Polymer 2012;4:275–795.
[84] Song K, Zhang Y, Meng J, Minus ML. Lubrication of poly(vinyl alcohol) chain orientation by carbon nanochips in composite tapes. J Appl Polym Sci 2012;127:2977–82.
[85] Jiang XL, Luo SJ, Sun K, Che XD. Effect of nucleating agents on crystallization kinetics of PET. eXPRESS Polym Lett 2007;1(4):245–51.
[86] Shaffer MS, Windle AH. Fabrication and characterization of carbon nanotube/poly(vinyl alcohol) composites. Adv Mater 1999;11(11):937–41.
[87] Zhang X, Liu T, Sreekumar TV, Kumar S, Moore VC, Hauge RH, et al. Poly(vinyl alcohol)/SWNT composite film. Nano Lett 2003;3(9):1285–8.
[88] Qian D, Dickey EC, Andrews R, Rantell T. Load transfer and deformation mechanisms in carbon nanotube-polystyrene composites. Appl Phys Lett 2000;76(20):2868–70.
[89] Strano M, Moore VC, Miller MK, Allen M, Haroz E, Kittrell C, et al. The role of surfactant adsorption during ultrasonication in the dispersion of single-walled carbon nanotubes. Nanosci Nanotechnol 2003;3:81–6.
[90] Ausman K, Piner R, Lourie O, Ruoff R. Organic solvent dispersions of single-walled carbon nanotubes: toward solutions of pristine nanotubes. J Phys Chem B 2000;104:8911–5.
[91] Valentini L, Biagiotti J, Kenny JM, Santucci S. Effect of single-walled carbon nanotubes on the crystallization behaviour of polypropylene. J Appl Polym Sci 2003;87(4):708–13.
[92] Leelapornpisit W, Ton-That M-T, Perrin-Sarazin F, Cole KC, Denault J, Simard B. Effect of carbon nanotubes on the crystallization and properties of polypropylene. J Polym Sci B Polym Phys 2005;43:2445–53.
[93] Haggenmueller R, Fischer JE, Winey KI. Single wall carbon nanotube/polyethylene nanocomposites: nucleating and templating polyethylene crystallites. Macromolecules 2006;39(8):2964–71.
[94] Kim JY, Park HS, Kim SH. Unique nucleation of multi-walled carbon nanotube and poly(ethylene 2,6-naphthalate) nanocomposites during non-isothermal crystallization. Polymer 2006;47:1379–89.
[95] Li L, Li CY, Ni C. Polymer crystallization-driven, periodic patterning on carbon nanotubes. J Am Chem Soc 2006;128(5):1692–9.
[96] Asadunezhad A, Khonakdar HA, Scheffler C, Wagenknecht U, Heinrich G. Poly(ethylene succinate)/single-walled carbon nanotube composites: a study on crystallization. Polym Bull 2013;70(12):3463–74.
[97] Wang W, Haung Z, Laird ED, Wang S, Li CY. Single-walled carbon nanotube nanoring induces polymer crystallization at liquid/liquid interface. Polymer 2015;54(24):1–9.
[98] Zhang Q, Lippits DR, Rasogi S. Dispersion and rheological aspects of SWNTs in ultrahigh molecular weight polyethylene. Macromolecules 2006;39(2):658–66.
[99] Parveen S, Rana S, Fangueiro R. A review on nanomaterial dispersion, microstructure, and mechanical properties of carbon nanotube and nanofiber reinforced cementitious composites. J Nanomater 2013;710175:1–19.
[100] Jogi BF, Sawant M, Kulkarni M, Brahamkar PK. Dispersion and performance properties of carbon nanotubes (CNTs) based polymer composites: a review. J Encapsul Adsorption Sci 2012;2:69–78.
[101] Kim SW, Kim T, Kim YS, Choi HS, Lim HJ, Yang SJ, et al. Surface modifications for the effective dispersion of carbon nanotubes in solvents and polymers. Carbon 2012;50:3.
[102] Ausman KD, Piner R, Lourie O, Ruoff RS, Korobov M. Organic solvent dispersions of single-walled carbon nanotubes: toward solutions of pristine nanotubes. J Phys Chem 2000;104(38):8911–5.
[103] Vaisman L, Marom G, Wagner HD. Dispersions of surface-modified carbon nanotubes in water-soluble and water-insoluble polymers. Adv Funct Mater 2006;16:357–63.
[104] Chen H, Muthuraman H, Stokes P, Zou J, Liu X, Wang J, et al. Dispersion of carbon nanotubes and polymer nanocomposite fabrication using trifluoroacetic acid as a co-solvent. Nanotechnology 2007;18:1–9.
[105] Mao X, Rutledge GC, Hatton TA. Polyvinylferrocene for noncovalent dispersion and redox- controlled precipitation of carbon nanotubes in nonaqueous media. Langmuir 2013;29:9626–34.

[106] Sahoo NG, Rana S, Cho JW, Li L, Chan SH. Polymer nanocomposites based on functionalized carbon nanotubes. Prog Polym Sci 2010;35:837–67.
[107] Galpaya D, Wang M, Liu M, Motta N, Waclawik E, Yan C. Recent advances in fabrication and characterization of graphene-polymer nanocomposites. Graphene 2012;1(2):30–49.
[108] Chung DDL. Exfoliation of graphite. J Mater Sci 1987;22:4190–8.
[109] Carotenuto G, Romeo V, Cannavaro I, Roncato D, Martorana B, Gosso M. Graphene-polymer composites. Mater Sci Eng 2012;40(012018):1–6.
[110] Stankovich S, Dikin DA, Piner RD, Kohlhaas KA, Kleinhammes A, Jia Y, et al. Synthesis of graphene-based nanosheets via chemical reduction of exfoliated graphite oxide. Carbon 2007;45:1558–65.
[111] Yakovlev AV, Finaenov AI, Zabud'kov SL, Yakovleva EV. Thermally expanded graphite: synthesis, properties, and prospects for use. Russ J Appl Chem 2006;79(11):1741–51.
[112] Celzard A, Mareche JF, Furdin G. Modelling of exfoliated graphite. Prog Mater Sci 2005;50:93–179.
[113] Loryuenyong V, Totepvimarn K, Eimburanapravat P, Boonchompoo W, Buasri A. Preparation and characterization of reduced graphene oxide sheets via water-based exfoliation and reduction methods. Adv Mater Sci Eng 2013;2013(923403):1–5.
[114] Park S, Ruoff RS. Chemical methods for the production of graphenes. Nat Nanotechnol 2009;4:217–24.
[115] Li D, Müller MB, Gilje S, Kaner RB, Wallace GG. Processable aqueous dispersions of graphene nano sheets. Nat Nanotechnol 2008;3:101–5.
[116] Pan S, Aksay IA. Factors controlling the size of graphene oxide sheets produced *via* the graphite oxide route. ACS Nano 2011;5:4073–83.
[117] Gudarzi MM, Sharif F. Characteristics of polymers that stabilize colloids for the production of graphene from graphene oxide. J Colloid Interface Sci 2010;349:63–9.
[118] Qiu SL, Wang CS, Wang YT, Liu CG, Chen XY, Xie HF, et al. Effects of graphene oxides on the cure behaviours of a tetra-functional epoxy resin. eXPRESS Polym Lett 2011;5:809–18.
[119] Lomeda JR, Doyle CD, Kosynkin DV, Hwang W-F, Tour JM. Diazonium functionalization of surfactant-wrapped chemically converted graphene sheets. J Am Chem Soc 2008;130:16201–6.
[120] Gudarzi MM, Sharif F. Enhancement of dispersion and bonding of graphene-polymer through wet transfer of functionalized graphene oxide. eXPRESS Polym Lett 2012;6(12):1017–31.
[121] Notarianni M, Liu J, Mirri F, Pasquali M, Motta N. Graphene-based supercapacitor with carbon nanotube film as highly efficient current collector. Nanotechnology 2014;25:1–7.
[122] Boukhvalov DW, Katsnelson MI, Lichtenstein AI. Hydrogen on graphene: electronic structure, total energy, structural distortions and magnetism from first-principles calculations. Phys Rev B 2008;77:035427/1–6.
[123] Reddy CD, Rajendran S, Liew KM. Equilibrium configuration and continuum elastic properties of finite sized graphene. Nanotechnology 2006;17:864–70.
[124] Nemes-Incze P, Osvatha Z, Kamarasb K, Biro LP. Anomalies in thickness measurements of graphene and few layer graphite crystals by tapping mode atomic force microscopy. Carbon 2008;46:1435–42.
[125] Lueking AD, Gutierrez HR, Fonseca DA, Dickey E. Structural characterization of exfoliated graphite nanofibers. Carbon 2007;45(4):751–9.
[126] Kim H, Macosko CW. Morphology and properties of polyester/exfoliated graphite nanocomposites. Macromolecules 2008;47:3317–27.
[127] Zhang D, Yan T, Shi L, Peng Z, Wen X, Zhang J. Enhanced capacitive deionization performance of graphene carbon nanotube composites. J Mater Chem 2012;22(29):14696–704.
[128] Chen J, Zheng X, Miao F, Zhang J, Cui X, Zheng W. Engineering graphene/carbon nanotube hybrid for direct electron transfer of glucose oxidase and glucose biosensor. J Appl Electrochem 2012;42:875–81.
[129] Cheng Q, Tang J, Ma J, Zhang H, Shinya N, Qin L-C. Graphene and carbon nanotube composite electrodes for super capacitors with ultra-high energy density. Phys Chem Chem Phys 2011;13:17615–24.
[130] Yen M-Y, Hsiao M-C, Liao S-H, Liu P-I, Tsai H-M, Ma CCM, et al. Preparation of graphene/multi-walled carbon nanotube hybrid and its use as photo-anodes of dry-sensitized solar cell. Carbon 2011;49:3597–606.

[131] Parker CB, Raut S, Brown B. Three-dimensional arrays of graphenated carbon nanotubes. Mater Res Soc 2012;27(7):1046–53.
[132] Stoner BR, Raut AS, Brown B, Parker CB, Glass JT. Graphenated carbon nanotubes for enhanced electrochemical double layer capacitor performance. Appl Phys Lett 2011;99(18):183104.
[133] Yu K, Lu G, Bo Z, Mao S, Chen J. Carbon nanotube with chemically bonded graphene leaves for electronic and optoelectronic applications. J Phys Chem Lett 2011;132(13):1556–62.
[134] Tian G-L, Zhao M-Q, Yu D, Kong X-Y, Haung JQ, Zhang Q, et al. Nitrogen-doped graphene/carbon nanotube hybrids: in situ formation on bifunctional catalysts and their superior electrocatalytic activity for oxygen evolution/reduction reaction. Small 2014;10(11):2251–9.
[135] Wimalasiri Y, Zou L. Carbon nanotube/graphene composite for enhanced capacitive deionization performance. Carbon 2013;59:464–71.
[136] Pham K-C, Chua DHC, Maphail DS, Wee ATS. The direct growth of graphene-carbon nanotube hybrids as catalyst support for high-performance PEM fuel cells. ECS Electrochem Lett 2014;3(6):F37–40.
[137] Acik M, Chabal YJ. Nature of graphene edges: a review. Jpn J Appl Phys 2011;50:1–16.
[138] Hong-tao C, Zhou O, Stoner BR. Deposition of aligned bamboo-like carbon nanotubes via microwave plasma enhanced chemical vapor deposition. J Appl Phys 2000;88(10):6072–4.
[139] Stoner Brian R, Glass JT. Carbon nanostructures: a morphological classification for charge density optimization. Diam Relat Mater 2012;23:130–4.
[140] Seo TH, Park AH, Park S, Kim YH, Lee GH, Kim MJ, et al. Direct growth of GaN layer on carbon nanotube-graphene hybrid structure and its application for light emitting diodes. Sci Rep 2015;5(7747):1–7.
[141] Dong P, Zhu Y, Zhang J, Hao F, Wu J, Lei S, et al. Vertically aligned carbon nanotubes/graphene hybrid electrode as a TCO- and Pt-free flexible cathode for application in solar cells. J Mater Chem A 2014;2:20902–7.
[142] Jesion I, Skibniewskip M, Skibniewska E, Strupiński W, Szulc-Dąbrowska L, Krajewska A, et al. Graphene and carbon nanocompounds: biofunctionalization and applications in tissue engineering. Biotechnol Biotechnol Equip 2015;29:1–8. http://dx.doi.org/10.1080/13102818.2015.1009726.
[143] Fan X, Jiao G, Gao L, Jin P, Li X. The preparation and drug delivery of a graphene–carbon nanotube–Fe_3O_4 nanoparticle hybrid. J Mater Chem B 2013;20(1):2658–64.